

PERFORMANCE LIMITS OF MICROWAVE OSCILLATORS WITH COMBINED STABILIZATION

D. P. Tsarapkin, and N. A. Shtin

MPEI, 14 Krasnokazarmennaya str., Moscow, 111250, Russia; E-mail: tsarap@srv-vmss.mpei.ac.ru

Abstract — As shown first in Ref. 1, an X-band microwave oscillator stabilized with a room temperature sapphire "whispering gallery" mode disk resonator used both as an oscillator feedback loop band-pass filter and a disperse element of a frequency discriminator of an additional frequency control system can provide ultra-low close-in phase noise approaching -150 dBc/Hz at 1 kHz offset.

This paper deals with performance limits of that oscillator scheme. Two-channel interferometric frequency discriminators (IFDs) is shown to have no potential advantages in comparison with the basic case where a circulator picks out a wave reflected from a near critically coupled resonator.

Two new IFD configurations providing the lower oscillator phase noise floor are described. The improvement is got by means of replacing the 3-dB hybrid in known IDF with a traveling wave directional filter using distributed coupling with the "whispering gallery" resonator that eliminates power loss.

As expected, the phase noise limit can be lowered up to -(160...165) dBc/Hz at 1 kHz offset.

Keywords — Ultra-low phase noise, microwave oscillator.

1. INTRODUCTION

Design of ultra-low phase noise microwave master oscillators remains a challenging problem in respect of new radars and some other modern coherent systems. This topic has received much attention in recent years as evidenced by a large number of publications. One of the best technical solutions, first published in Ref. 1, is represented by a room temperature microwave oscillator doubly stabilized with a sapphire "whispering gallery" mode disk resonator used both as a narrow-band filter of an oscillator positive feedback loop and a disperse element of a frequency discriminator (FD) of an additional frequency control system (FCS). As shown in Ref. 1, such X-band transistor sources can provide close-in phase noise approaching -150 dBc/Hz at 1 kHz offset. The following experiments by

E. N. Ivanov, M. E. Tobar et al. proved this theoretical estimation [Ref. 2]. However, all further attempts to gain greatly the result failed practically [Ref. 3].

Phase noise of the oscillator with combined stabilization arises due to noisy elements in oscillator circuitry comprising (Fig. 1) a whispering gallery resonator (WGR; "Res." in Fig. 1), a sustaining amplifier (SA), a circulator based "reflected wave extractor", a phase detector (PD), one or two auxiliary microwave low noise limiting amplifiers (LNLA) A_1 , A_2 in front of the PD, a low frequency amplifier (LFA), a voltage controlled phase shifter (VCP) and some additional components. The noise can be written as

$$\mathcal{L}(F) = \mathcal{L}_{FCS}(F) + \mathcal{L}_{os}(F) / K_{FCS}^2(F). \quad (1)$$

Here $\mathcal{L}(F)$ — total SSB oscillator phase noise; F — a Fourier frequency; \mathcal{L}_{FCS} — FCS intrinsic phase noise; \mathcal{L}_{os} — phase noise of a free running oscillator; $K_{FCS}(F)$ — modulus of the FCS open loop frequency response. Thus, in the case of FCS loop gain being high enough the phase noise is limited mainly by intrinsic noise sources in the circulator, LNLA and PD forming FD together with the noiseless WGR.

At room temperature sapphire WGR self Q -factor, Q_o , is equal $\approx 2 \times 10^6 / f$ if the operating frequency f is taken in gigahertz. Put loaded Q -factor $Q_L \sim Q_o / 2$ and $f \sim 10$ GHz. Then the expected WGR's bandwidth is about 100 kHz. It follows, analyzing close-in phase noise one can ignore noise alteration between different oscillator sections and use the shorter Leeson's formula for filtered phase noise at the SA input:

$$\mathcal{L}_{os}(F) = \frac{1}{2} S_{sa}(F) \cdot (B_o / q_L F)^2, \quad \text{rad}^2/\text{Hz}. \quad (2)$$

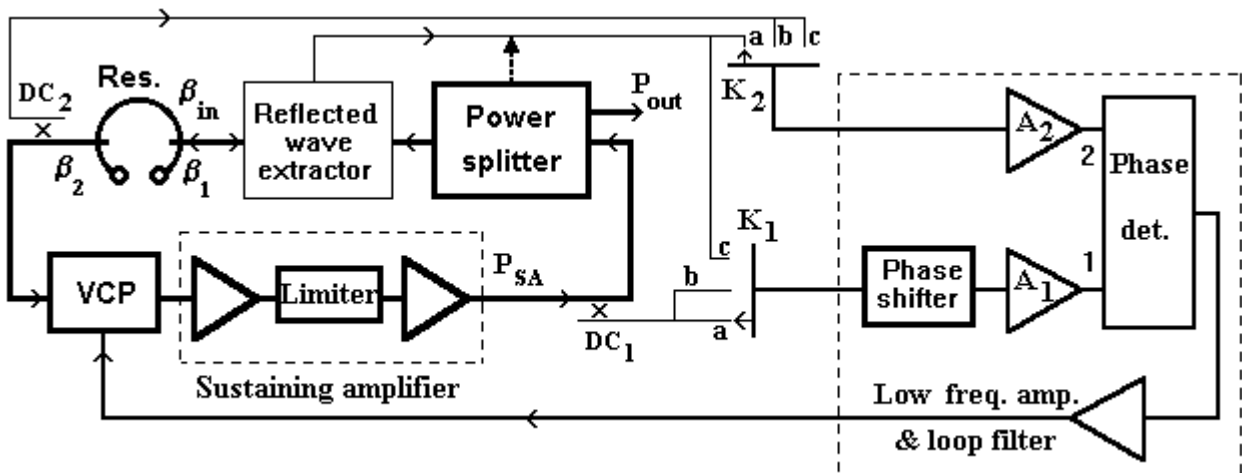


Figure 1. Generalized block diagram of the oscillator with combined stabilization. Three main configurations (a, b, c) are possible.

Here S_{SA} — phase noise of the sustaining amplifier;
 $q_L = Q_L/Q_o$ — a normalized loaded Q -factor;
 $B_o = f/2Q_o$ — a half bandwidth of the unloaded resonator.

High quality microwave BJT amplifiers have $S_{SA} = -145... -155$ dBc/Hz at 1 kHz offset. Let $S_{SA} = -150$ dBc/Hz. Then (2) gives for the free running oscillator an estimation $\mathcal{E}_{os}(1 \text{ kHz}) \approx -119$ dBc/Hz which coincides with experimental data. Hence, to get $\mathcal{E}(1 \text{ kHz}) \approx -150$ dBc/Hz at the output the FCS must provide around 30 dB noise suppression. It is not too much. So the only reason that can impede to reach the desired ultra-low phase noise level lies in intrinsic FCS noise.

The oscillator phase noise floor $\mathcal{E}_{fl} = \mathcal{E}_{FCS}$. It is convenient to add the LFA noise to the PD one, attach the VCP noise to SA and cancel the LNLA at the reference PD input. Then, as shown in Ref. 1,

$$\mathcal{E}_{fl}(F) = 1/2(S_{int} + S_{LNLA} + V_{PD}/K_{PD}^2) \cdot (B_o/q_e F)^2. \quad (3)$$

Here S_{int} — a spectral density of intrinsic phase noise of the interferometer (microwave bridge), rad^2/Hz ; S_{LNLA} — the same for LNLA, V_{PD} — the same for PD in terms of its output voltage fluctuations, V^2/Hz ; $K_{PD} = 0.5-0.9 \text{ V/rad}$ — a PD phase-to-voltage conversion factor (Refs 4, 5); q_e — normalized effective Q -factor describing gain in taken at a resonance steepness of the “bridge” output phase versus frequency response in comparison with the analog quantity for an unloaded WGR. Eqn. (4) reflects a fact the FD in Fig. 1 reacts to frequency fluctuations via frequency-to-phase conversion in WGR and subsequent measurement of the arising phase disturbances. According to Ref. 4

$$V_{PD}(F) \approx 10^{-14} / F + 10^{-17}, \quad V^2/\text{Hz}. \quad (4)$$

A double-balanced PD has a minimal noise-to-signal ratio when incoming power is about the same at both inputs and an every Schottky diode consumes 1-3 mW. To meet the optimizing conditions the gain of the corresponding LNLA must automatically follow the interferometer output when network parameters are being changed.

2. INTERFEROMETER ANALYSIS

The main interferometer characteristics, which we are interested in, are the amplitude transfer function $K_{int} = U_{int out}/U_{inc}$; the phase conversion factor $K_{ph} = |d(\arg K_{int})/df|$, rad/Hz ; the intrinsic phase noise. Here U_{inc} , $U_{int out}$ — complex amplitudes of the incident and output interferometer signals accordingly.

2.1 Basic single channel interferometer

The most intensive phase conversion is provided by carrier suppression (cases “a” and “c” in Fig. 1) [Refs 1-5]. The classic network realizing the case “a” is shown in Fig. 2. It has

$$K_{int} = (p + 1 - \beta_{in}) / (p + 1 + \beta_{in}), \quad (5)$$

where $p = j\xi$; $\xi = (f/f_{res} - f_{res}/f)Q_o/(1+\beta_2)$; f_{res} — a resonant frequency; $\beta_{in} = \beta_1/(1+\beta_2)$ — a normalized WGR input impedance due to couplings β_1 , β_2 . Put $f = f_{res}$, designate $|K_{int}(f_{res})| = K_o = |1 - \beta_{in}|(1 + \beta_{in})^{-1}$, $K_{ph}(f_{res}) = K_{pho} = q_e/B_o = 2\beta_{in}[|1 - \beta_{in}|(1 + \beta_{in})(1 + \beta_2)B_o]^{-1}$ and introduce a figure of merit

$$T_o = K_o \cdot q_e = 2\beta_{in}(1 + \beta_{in})^{-2}(1 + \beta_2)^{-1} \quad (6)$$

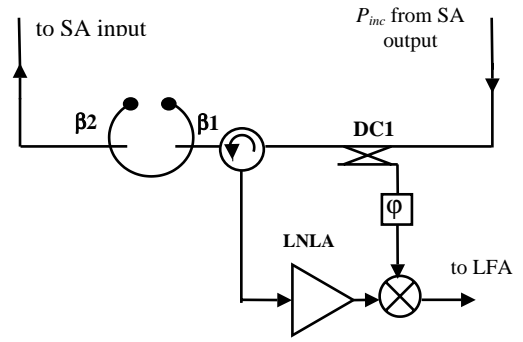


Figure 2. Schematic of the basic single channel interferometer.

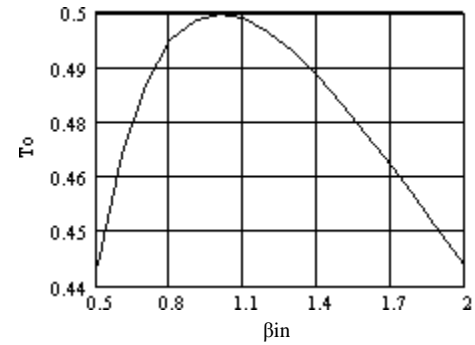


Figure 3. T_o vs. β_{in} plot for the one-channel interferometer.

which takes into account both the amplitude and phase transfer. $T_o(\beta_{in})$ has a flat optimum at $\beta_{in} = 1$; $T_{o max} = 0.5$ (Fig. 3).

Consider now impact of the LNLA and circulator phase noise on the oscillator noise floor. The term S_{LNLA} in (3) is equal $kTN_{LNLA}/P_{inc}K_o^2$ where N_{LNLA} and P_{inc} represent, accordingly, the LNLA noise figure and the microwave power incident on WGR. Hence, this part of the total \mathcal{E}_{fl} gives

$$\mathcal{E}_{fl}^{LNLA}(F) = [kTN_{LNLA}(F)/2P_{inc} \cdot T_o^{-2} \cdot (B_o/F)^2]. \quad (7)$$

The answer is straightforward: the more T_o the less residual phase noise. If $T_o \approx T_{o max}$, $P_{inc} = 50 \text{ mW}$, $B_o = 40 \text{ kHz}$ then $\mathcal{E}_{fl}^{LNLA}(1 \text{ kHz}) = -156 + N_{LNLA}$, dBc/Hz. The HEMT X-band amplifier having in the μW -regime $N_{LNLA}(1 \text{ kHz}) \approx 1 \text{ dB}$ is used successfully in Refs 2, 3 as LNLA. New low noise SiGe HBTs demonstrate the same or even lower N_{LNLA} being excited by 1 mW input (Ref. 6). It opens a possibility to lower \mathcal{E}_{fl}^{LNLA} via P_{inc} increase and, in parallel, optimize a PD regime.

On the contrary, as far as the effect of circulator noise on \mathcal{E}_{fl} is concerned there is obvious lack of understanding among specialists. The approximate formula in Ref. 1 (slightly modified here) for spectral density of ferrite circulator intrinsic phase noise with respect to the isolating output is

$$S_{cir}(F) \approx S_{cirs}(F) \cdot (3 + \chi \cdot \Gamma_o^{-2}) \quad (8)$$

where S_{cirs} — the DSB phase noise for a signal passing between adjacent circulator inputs in forward direction; $\Gamma_o = |1 - \beta_{in}|(1 + \beta_{in})^{-1}$ — a reflection coefficient at $f = f_{res}$; $\chi = 0.25-1$. Eqn. (8) is based on a view of the circulator like a kind of an interferometer with intrinsically noisy arms. It follows, the

multiplicative interferometric noise at the isolated output always exists. This noise is proportional to incoming power, has 1/F spectrum, but acts as additive one. The experimental data by the UWA team (Ref. 3: -183 dBc/Hz at 1 kHz offset for DSB noise) describe namely S_{cirs} , which is far from resulting S_{cir} if β_{in} is close to unity. Thus, a ferrite circulator with phase noise given by (8) yields a part of the total IFD noise floor

$$\mathcal{L}_{fl}^{cir}(F) = \mathcal{L}_{cirs}(F) \cdot (3 + \chi \cdot \Gamma_o^{-2}) \cdot (B_o/q_e F)^2. \quad (9)$$

In the case of $\Gamma_o = 0.01$ (40-dB carrier suppression) the second term in (8)-(9) gives 28...40 dB noise rise depending on the coefficient χ . For data in Ref. 3 where much more $\Gamma_o = 0.21$ is used, $\mathcal{L}_{fl}^{cir}(1 \text{ kHz}) = -164.4 + (9.4...14) \text{ dBc/Hz}$. Experimentally, $\mathcal{L}(1 \text{ kHz}) = -148 \text{ dB/Hz}$. So, it is wise to choose $\chi = 1$ as in Ref. 1 what yields $\mathcal{L}_{fl}^{cir}(1 \text{ kHz}) = -150.4 \text{ dBc/Hz}$.

For $\Gamma_o \ll 1$, bearing in mind $\chi = 1$ and Fig. 3, (9) is reduced to

$$\mathcal{L}_{fl-limit}^{cir}(F) = \mathcal{L}_{cirs}(F) \cdot (2B_o/F)^2. \quad (10)$$

With $\mathcal{L}_{cirs} = -186 \text{ dBc/Hz}$ and $B_o = 23.7 \text{ kHz}$ (Ref. 3 case) $\mathcal{L}_{fl-limit}^{cir}(1 \text{ kHz}) = -152.5 \text{ dBc/Hz}$. It is the key restriction.

2.2 Two-channel interferometers using a circulator

One can try to overcome the limit (10) in a two-channel interferometer where it is possible to fix first a rather big reflected signal and then tune the needed degree of carrier suppression with help of the second channel. Two realizations of such a network are drawn in Figs 4, 5. In Fig. 4 (Int-2A) the second branch uses via DC2, DC3 a part of incoming power, in Fig. 5 (Int-2B) - some part of power passed through WGR.

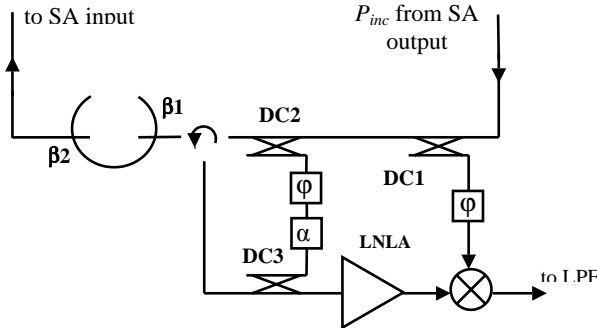


Figure 4. Schematic of the two-channel interferometer "A".

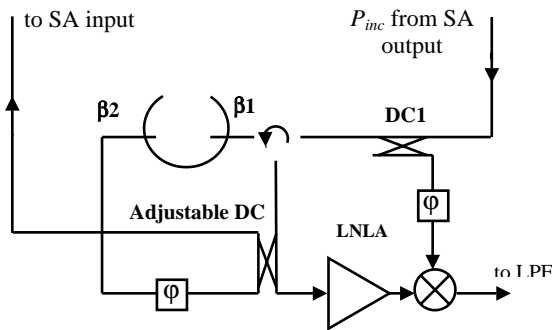


Figure 5. Schematic of the two-channel interferometer "B".

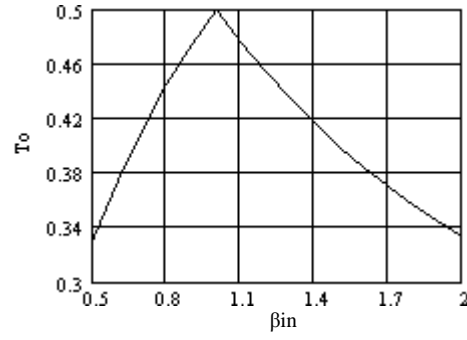


Figure 6. T_o vs. β_{in} plot for the two-channel interferometer "Int-2A" in Fig. 4.

The transfer functions of both two-channel interferometers look like (5). It is quite expected as Int-2A and Int-2B realize the same simple bridge circuit having one zero and one pole. In particular,

$$K_{Int-2A}(p) = 1 - c^2 \cdot \frac{p+1-\beta_{in}}{p+1+\beta_{in}} - c^2 \quad (11)$$

if DC2 and DC3 are identical. The coefficient c describes here power distributions between DC outputs. To balance bridge, $c = \sqrt{(1-\beta_{in})/2}$ for $\beta_{in} \leq 1$ and $c = \sqrt{(\beta_{in}-1)/2\beta_{in}}$ for $\beta_{in} \geq 1$. With these conditions met

$$T_o = \frac{2\beta_{in}}{(1+\beta_{in})^2(1+\beta_2)} \cdot (1-c^2). \quad (12)$$

Eqn. (12) differs from eqn. (6) by the last term that characterizes additional power losses in the directional couplers. It results the curve in Fig. 6 falls down steeper in comparison with the basic case in Fig. 3 when β_{in} deviates from unity. As for the Int-2A phase noise, it stays the same as before just due to the intrinsic circulator noise exposes itself as additive. Detailed analysis of Int-2A can be found in Ref. 3. In practice this interferometer is applied, mainly, as a useful tool to compensate circulator leakage and balance the microwave bridge.

Int-2B is similar to Int-2A in main properties but demands only one additional DC. Eqns (11)-(12) are replaced here with

$$K_{Int-2B} = \sqrt{1-c^2} \cdot \frac{p+1-\beta_1+\beta_2}{p+1+\beta_1+\beta_2} + c \cdot \frac{2\sqrt{\beta_1\beta_2}}{p+1+\beta_1+\beta_2},$$

$$c = \frac{1+\beta_2-\beta_1}{\sqrt{(1+\beta_2-\beta_1)^2 + 4\beta_1\beta_2}}; \quad (13)$$

$$T_o = \frac{2\beta_1\sqrt{1-c^2} - 2c\sqrt{\beta_1\beta_2}}{(1+\beta_1+\beta_2)^2} \quad (14)$$

accordingly. Unfortunately, a part of the reflected signal coming to the left side output Int-2B branch through the adjustable DC effects the oscillator positive feedback loop transfer function, lowers effective Q-factor and may even cause steady-state regime instability. Some more examples of two-channel interferometers are described in Ref. 7.

2.3 Interferometers without a circulator

A ferrite circulator in the IDF network extracts a wave reflected from a high-Q resonator. At the same time namely the circulator intrinsic noise limits an achievable phase noise floor. Thus, it looks reasonable to replace the circulator by another device performing needed operation but having no excess noise.

In 1994 D. P. Tsarapkin suggested to use in this function a 3-dB hybrid splitting a half of generated power to an oscillator load (Ref. 1). At the first sight, such a solution decreases T_o , and so \mathcal{L}_{ff}^{LNA} , by 6 dB. Fortunately, the real loss is 1...3 dB less as separation of a substantial part of SA output is compulsory anyway. Going back to (7), we conclude that with SA providing 250-500 mW output power there is real perspective to build the oscillator having $\mathcal{L} = -(158...160)$ dBc/Hz at 1 kHz offset.

To avoid the power loss leading to noise degradation one can replace the 3-dB hybrid with a WGR based traveling wave directional filter (TWDF; Fig. 7). Due to distributed coupling in TWDF the interferometer keeps all advantages of the basic configuration in Fig. 2 as far as T_o is concerned. Our proposal has the edge on the patented variant in Ref. 8 as ours eliminates power loss of the information signal in the hybrid coupler placed before LNA in Fig. 9 of Ref. 8.

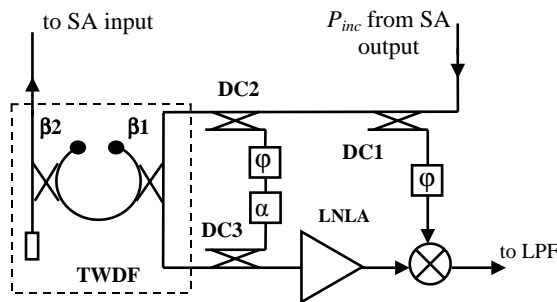


Figure 7. Schematic of the two-channel TWDF interferometer.

The next network in Fig. 8 is a result of spreading the TWDF conception on the interferometer in Fig. 2 of Ref. 7. With $\beta_1 = \beta_2 = 0.5$, $\beta_{SA} \sim 0.1$ additional gain in T_o could be about 1.5 dB.

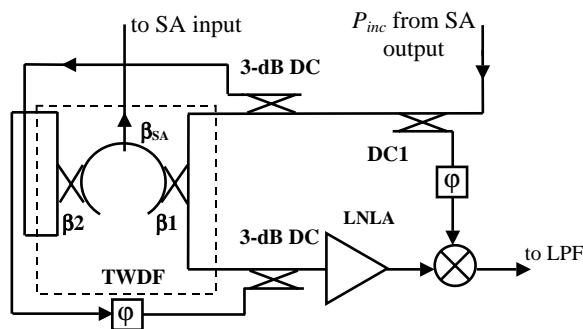


Figure 8. Schematic of the advanced TWDF interferometer.

Summarizing, we come to a conclusion that optimistic estimation gives here $\mathcal{L}(1 \text{ kHz}) \sim -165$ dBc/Hz as a low limit.

CONCLUSION

Intrinsic noise of a ferrite circulator into a microwave interferometer network limits available phase noise of a room temperature X-band WGR oscillator with combined stabilization by a value close to -150 dBc/Hz at 1 kHz offset.

The only way to further phase noise improvement lies in replacing the circulator as an element of carrier suppression circuitry with a noiseless reciprocal device, e.g. a 3-dB hybrid junction. The most promising solution consists in using for this function of a WGR based traveling wave directional filter. The expected phase noise limit can be lowered here up to $-(160...165)$ dBc/Hz at 1 kHz offset.

REFERENCES

1. D. P. Tsarapkin, «Low Phase Noise Sapphire Disk Dielectric Resonator Oscillator with Combined Stabilization», in *Proc. 1994 IEEE Int. Freq. Contr. Symp.*, pp. 451-458.
2. E. N. Ivanov, M. E. Tobar and R. A. Woode, «Advanced Phase Noise Suppression Technique for Next Generation of Ultra Low-Noise Microwave Oscillators», in *Proc. 1995 IEEE Int. Freq. Contr. Symp.*, pp. 314-320.
3. J. G. Hartnett, M. E. Tobar, and E. N. Ivanov, «Novel Interferometric Frequency Discriminators for Low Noise Microwave Applications», *IEEE Trans. UFFC*, vol. 45, no. 6, pp. 1526-1536 (1998).
4. F. L. Walls, C. M. Felton, and T. D. Martin, «High spectral purity X-band source», in *Proc. 44th Annual Freq. Contr. Symp.*, 1990, pp. 542-548.
5. M. M. Driscoll and R. W. Weinert, «Low noise, microwave signal generation using cryogenic, sapphire dielectric resonators: An update», in *Proc. 46th Annual Freq. Contr. Symp.*, 1992, pp. 157-162.
6. G. Niu, Z. Jin, J.D. Cressler, et al., «Transistor Noise in SiGe HBT RF Technology», *IEEE Journal of Solid-State Circuits*, vol. 36, no. 9, pp. 1424-1427 (2001).
7. J. G. Hartnett, M. E. Tobar, and E. N. Ivanov, «Novel Interferometric Frequency Discriminators for Low Noise Microwave Applications», *IEEE Trans. UFFC*, vol. 48, no. 3, pp. 743-749 (2001).
8. E. N. Ivanov, M. E. Tobar, P. Blondy, D. Cros, P. Guilon, «High-Q Whispering Gallery Travelling Wave Resonators for Oscillator Frequency Stabilization», in *Proc. 1999 Joint Meeting EFTF-IEEE IFCS*, 1999, pp. 589-592.